Femtosecond laser rapid prototyping of nanoshells and suspending components towards microfluidic devices

Dong Wu, Qi-Dai Chen, Li-Gang Niu, Jian-Nan Wang, Juan Wang, Rui Wang, Hong Xia and Hong-Bo Sun*

Microfluidic researches are now resorting to advanced micro-nanoprocessing technologies for production of more functional "lab-on-a-chip" systems. However, two-photon polymerization (TPP), a powerful designable micro-nanofabrication approach, has not been put to use on the exciting field, largely due to the difficulties in forming buried channels. Here, we solve the problem by TPP prototyping of nanoshells, for which the usage of the negative tone resin SU-8 is found critical. The fabrication efficiency improved by orders of magnitude, together with the prospect of integration of movable micro-mechanical and optical components into the chip would make TPP a promising enabling tool for the micro-analytical systems. Finally, a 25 μm length functional microvalve in a microfluidic channel was rapidly realized and its "ON" and "OFF" states were tested.

Interests in scaled-down analytical processes with the concept of microfluidics is motivating the rapid progress of "lab-on-a-chip" systems,[1–3] by which biological and chemical assays are being conducted more rapidly, at lower cost and with smaller amount of samples. Recently, the efforts in the field fall into two categories:[2,3] (a) development of less expensive materials and technical routes for industrial applications, as represented by injection molding, casting, hot embossing and thermal forming; (b) pursuit of higher functional chips to explore new phenomena in complex biological and chemical microsystems, which are otherwise not possible to access. Following the second line, ultraviolet (UV), e-beam, X-ray lithography, stereolithography and nanoimprint are widely used,[2,3] which are, however, not cost-effective (various lithographies) or insufficient in fabrication accuracy (stereolithography). Femtosecond laser direct writing by two-photon photopolymerization (TPP) of resins[4–7] is ideal due to its advantages such as nanometre spatial resolution, three-dimensional (3D) prototyping capability, and the diversity of usable materials. As a designable nanofabrication method, TPP has been applied to produce micro-optical and mechanical components such as high efficiency Fresnel zone plates,[8] fractal zone plates[9] aspheric micro-lens array, and magnetically-driven micro-oscillators.[10] Such a powerful technology, however, has not been put to use on fabrication of "lab-on-a-chip". The underlying reason lies in that a chip usually consists of various channels buried in a solid background and functional micro-machines.[11] Point-by-point writing leads to unreasonably low fabrication efficiency. In this technical note, we solve the problem by pinpoint TPP scanning only the surface layer (shell) comprising of a chip while the background is either removed by solvents or is solidified by additional ultraviolet exposure. The use of the solid photopolymer SU-8 is found critical for the formation of thin shells, as well as for the production of

suspending components, essential for advanced functions of a lab-on-a-chip system.

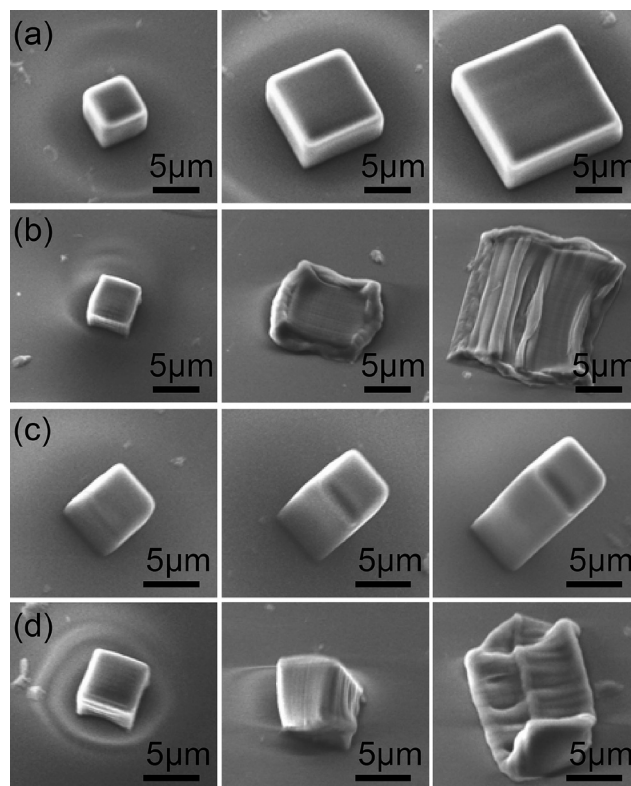Fig. 1(a) shows tilted-view scanning electron microscopic (SEM) images of cuboids with different side lengths of 4 μm,

Fig. 1 SEM images of cuboids fabricated by TPP of SU-8 and NOA 61 through nanoshell definition. (a), (c) Structures from SU-8 and (b), (d) from NOA 61. For (a) and (b), the side lengths of the cuboids are 4 μm, 8 μm, and 12 μm from the left to the right, while for structures (c) and (d), the bottom areas are kept 4 μm × 4 μm and the height increases from 4 μm, 8 μm to 12 μm from left to right.

State Key Laboratory on Integrated Optoelectronics, College of Electronic Science and Engineering, Jilin University, 2699 Qianjin Street, Changchun, 130023, China. E-mail: hbsun@jlu.edu.cn; Fax: +86 431 85168281; Tel: +86 431 85168281

8 μm and 12 μm, fabricated by TPP of commercial epoxy-based negative resin SU-8, which has been widely utilized for TPP fabrication.[12] The resin features high transmittance for light from the visible to the near infrared wavelengths, low volume shrinkage of polymerization, good mechanical properties and high thermal stability (degradation temperature ~380 °C), making it a good candidate for micro-nanostructures. A femtosecond laser pulse of 790 nm central wavelength, 120 fs pulse width, 80 MHz repetition rate was tightly focused by a ×100 oil immersion objective lens with a high numerical aperture ($NA = 1.4$) into the resin. The laser focal spot was scanned laterally by steering a two-galvano-mirror set and along the optical axis by a piezoelectric stage. The photoresist samples are prepared by spin-coating SU-8 films on microscopic cover slides. After evaporation of the solvent in a soft-bake step for 30 minutes at 95 °C, a 20 μm thick film is obtained. During the femtosecond laser direct writing according to preprogrammed patterns, acid is generated with a concentration following the distribution of the square of the light intensity. Then, the resin SU-8 was post-baked with a temperature ramp from 65 °C to 95 °C for ten minutes and the latent image was converted into a crosslinked solid skeleton by a cationic photoamplification. Finally, the sample was developed in the SU-8 developer for 60 minutes to remove the unsolidified resin.

The crosslinking degree determines the solubility of the exposed SU-8 in a developing solvent. Sufficiently illuminated resin remains whereas the underexposed resin is washed out. To improve the fabrication efficiency, we adopted the strategy of profile scanning,[13] which means that only the structure surface layer was defined by TPP. As can be seen from Fig. 1(a), there is no visible deformation in the three cuboids. For comparison, the process was repeated with the liquid resin NOA 61 [Fig. 1(b)]. Although no distortion is found from the 4 μm cuboid, deformation occurred when its size increased to 8 μm. The cuboid collapsed when the side length reached 12 μm. In both cases, the shells were defined by single-layer scanning, and the laser pulse energy was chosen to be approximately 1.1 times the TPP threshold for each resin,[10] which defined a layer thickness of around 300 nm. There are at least two factors responsible for the distortion. (a) First is the different phase status of resins. The unexposed inner portion for the SU-8 cuboid is of solid phase, which exerts a lesser force on the shell due to intermolecular attractions, while the NOA 61 cuboid shell has to withstand, more or less, the hydrostatic pressure caused by the weight of the resin. Furthermore, SU-8 has better mechanical strength, e.g., its elastic modulus is 4.5 GPa against 1.03 GPa for NOA 61.[14] (b) The second reason is related to the above, but more from ambient conditions. For liquid resins, the vibrations from developing and drying processes cause shock and acceleration and deform the fragile nanoshell by exerting it pulling, pushing, striking or capillary forces.

This effect has been further proved by fabricating high aspect-ratio structures with thinner shells, which are easier to be disturbed. The laser power was lowered to around 1.05 times the TPP thresholds, resulting in layer thickness of approximately 100 nm. For a fixed bottom cross-section of 4 μm × 4 μm, no distortion was observed in SU-8 cuboids of various heights, 4 μm, 8 μm and 12 μm [Fig. 1(c)]. In contrast, a slight deformation occurred starting from the 4 μm NOA 61 structure [Fig. 1(d)]. Although less indicative, if we defined an aspect ratio as the cuboid height divided by the entire side wall thicknesses (100 nm × 4), it is 48 for SU-8, the same level as that achieved from solid rods, 50,[15] while that for NOA 61 is less than 10.

The approach of TPP prototyping of SU-8 nanoshells is practically useful in, at least, two aspects. (a) Production of stand-alone shell structures. Shown in Fig. 2(a) and (b) are SEM images of an imagined astronomical observatory, consisting of a 40 μm diameter hemisphere with four 5 μm diameter holes, which is like the 3D microcages or microcontainers in microfluidic devices to encapsulate both nonliving and living objects and form 3D patterned microwells.[16] Due to lack of support by the inner fillings, the shell thickness was designed to be 800 nm, while that from NOA 61 requires at least 5 μm to stand. (b) The second is as those done in Fig. 2(c), i.e., the shell defines a contour of a larger structure, while the polymer below it was further solidified by single-photon exposure. In this case, the TPP exposure duration could be significantly shortened. The degree of efficiency increase depends on the specific structures: the larger the volume of the internal portion is, the more the saved exposure time becomes. For example, the micro lens array [Fig. 2(d)] bears a large surface area, for which the processing time was reduced from the previous 30 minutes to 4 minutes by TPP of the shell. With the same approach, the fabrication time of a 20 μm side length cuboid was significantly brought down from 133 minutes to 3 minutes, indicating a more than 40 times improvement.

These two kinds of nanoshell usage actually pointed out how the TPP technology may become important for fabrication of a "lab-on-a-chip". On one hand, walls consisting of a channel thin enough to produce economically and thick enough to resist leakage and mechanical damage, generally of the order of micrometres, could be directly depicted by TPP; on the other hand, the one-order thinner shells could be used to define the surface of the background, from which buried channels are naturally introduced as designed. As a test of concept, the
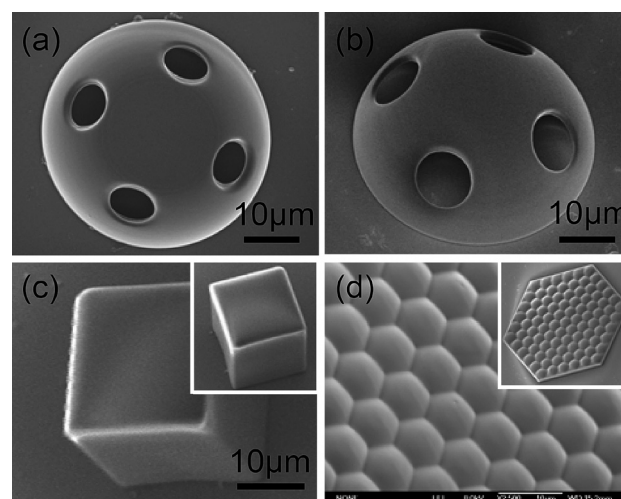

Fig. 2 Nanoshell structuring by TPP. (a), (b) Top-view and tilted-view SEM images of a stand alone hemisphere with holes. (c) A cuboid with large volume, whose fabrication time took only 3 minutes. (d) A 100% fill-factor hexagonal micro-lens array with large surface area, which was written in 3 minutes.

microfluidic device proposed by Jamil *et al.*[17] was reproduced, which was designed as a disk structure of 100 μm diameter and 15 μm height ([Fig. 3(b)]). A 3D filtration network with six 2 μm sized bores was designed for the separation function of impurity and cells with different sizes [Fig. 3(d)]. The version with stand-alone shells directly defining the device with walls [Fig. 3(a) and (c)] and that with buried channels created with the aid of additional ultraviolet exposure are both capable of functioning as designed. In the latter case, The TPP fabrication time is dramatically reduced from 20 hours to less than 30 minutes. The additional single-photon exposure duration, only if it is saturated, affects less the quality of resultant structures. Compared with the pioneering work based on positive tone photoresist done by Perry *et al.*,[11] the negative tone SU-8 is advantageous in spatial resolution of fabrication and functionalization of materials, and in the ease of fabricating functional moving parts.

Fabrication of well-defined untouched moving components is challenging because deformation induced by drift usually occurs in liquid resins. For SU-8, the choice of exposure condition is also essential, over exposure or insufficient exposure produce structures either strung together, such as the 2.5 μm radius rings in the left two images in Fig. 4(a), or elongated ones (the right two images) because of the insufficiency of mechanical strength of the polymerized skeleton. A 1.1 times of exposure threshold leads to structures with designed shape and size [Fig. 3(b) and (c)]. Not only they do stand well in air, but also move freely in solution [Fig. 4(d) and (e)]. Because of the femtosecond direct writing, all of the fixed and movable parts are rapidly realized by one-step two-photon polymerization of SU-8. Compared with other microfabrication technologies, such as Sandia Summit process, the femtosecond technology is very simple, rapid, and highly precise for the fabrication of 3D complicated micro-nanoscale functional micromachines. This shows the promising

Fig. 4 Movable devices. (a) Tilted-view SEM image of a chain structures consisting of 5 and 20 rings with inappropriate exposure conditions. (b) And (c) are well-defined structures. (d) And (e), movement of chains in solution.

prospect of TPP of SU-8 for producing functional devices like micro-pumps and microvalves in a lab-on-a-chip system.

To verify this thought, we fabricated a movable microvalve with single movement direction integrated in a microfluidic channel by one-step femtosecond direct writing, as shown in Fig. 5(a). From the tilted-view SEM image [Fig. 5(b)], the microvalve is 25 μm in length and 10 μm in height. It is composed of a fixed substrate, two rings and a big gate. It can only move in one direction due to the gate frame. When the water flows in the direction of the arrow [Fig. 5(c)], the gate freely opens, which is
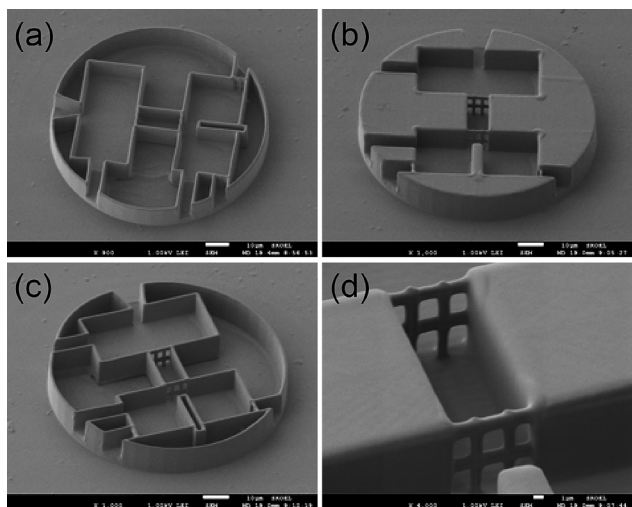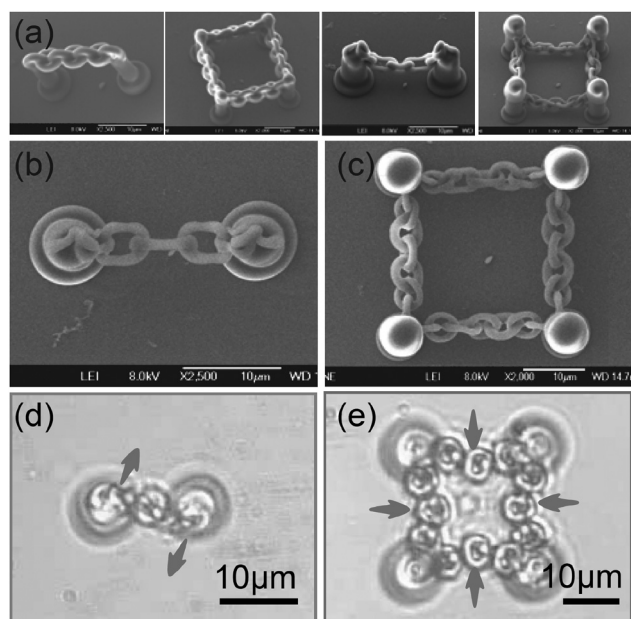

Fig. 3 A conceptual microfluidic device fabricated by TPP of SU-8. (a) Overall SEM view of the 3D microfluidic systems with 100 μm diameter disk and 15 μm height. Here, the internal portion of the background volume is solidified by additional ultraviolet exposure. (b) Two infiltration networks with six 2 μm sized bores. (c), (d) SEM images of the same microfluidic devices but consisting of stand alone shell as walls.
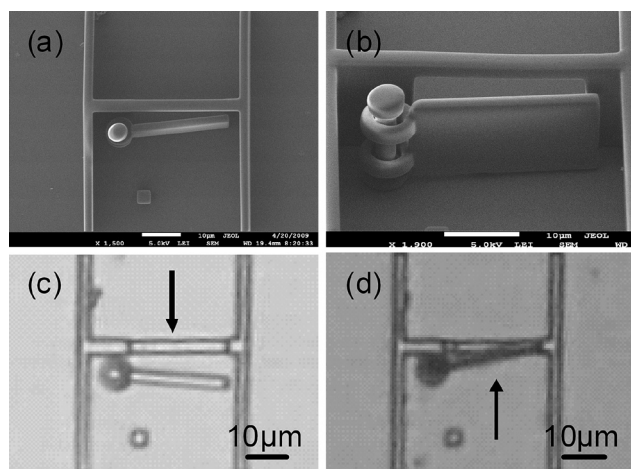

Fig. 5 Functional microvalve with a single direction. (a) Top-view SEM image of microfluidic channel and a 25 μm length movable microvalve. (b) 45°-tilted-view SEM image of the microvalve and the gate. (c) And (d) are the "OFF" and "ON" function under different water flow directions.

the "ON" state. In contrast, when the water comes from the opposite direction, the gate exhibits the "OFF" state.

In conclusion, the usage of nanoshells significantly improves the fabrication efficiency of microfluidic devices. This, together with the possibility of 3D integration of channels with micro-optical and mechanical components, makes TPP attractive for higher functional lab-on-a-chip systems.

References

1 H. Craighead, *Nature*, 2006, **442**, 387.
2 H. Andersson, *Sens. Actuat. B*, 2003, **92**, 315.
3 P. C. H. Li, *Microfluidic Lab-on-a-Chip for Chemical and Biological Analysis and Discovery*, CRC press, Tailor and Francis, New York, 2006.
4 S. Maruo, O. Nakamura and S. Kawata, *Opt. Lett.*, 1997, **22**, 132.
5 H. B. Sun and S. Kawata, *Adv. Polymer Sci.*, 2004, **170**, 169.
6 S. Kawata, H. B. Sun, T. Tanaka and K. Takada, *Nature*, 2001, **412**, 697.
7 S. H. Park, S. H. Lee, D. Y. Yang, H. J. Kong and K. S. Lee, *Appl. Phys. Lett.*, 2005, **87**, 154108.
8 Q. D. Chen, D. Wu, L. G. Niu, J. Wang, X. F. Lin, H. Xia and H. B. Sun, *Appl. Phys. Lett.*, 2007, **91**, 171105.
9 D. Wu, L. G. Niu, Q. D. Chen, R. Wang and H. B. Sun, *Opt. Lett.*, 2008, **33**, 2913.
10 J. Wang, H. Xia, B.-B. Xu, L.-G. Niu, D. Wu, Q.-D. Chen and H.-B. Sun, *Opt. Lett.*, 2009, **34**, 581.
11 W. H. Zhou, S. M. Kuebler, K. L. Braun, T. Y. Yu, J. K. Cammack, C. K. Ober, J. W. Perry and S. R. Marder, *Science*, 2002, **296**, 1106.
12 W. H. Teh, U. Durig, G. Salis, R. Harbers, U. Drechsler, R. F. Marhrt, C. G. Smith and H. J. Guntherodt, *Appl. Phys. Lett.*, 2004, **84**, 4095.
13 T. Tanaka, H. B. Sun and S. Kawat, *Appl. Phys. Lett.*, 2002, **80**, 312.
14 Data are from the catalogue of each product, either printed or from the homepage.
15 W. H. Teh, U. Durig, U. Drechsler, C. G. Smith and H. J. Guntherodt, *J. Appl. Phys.*, 2005, **97**, 054907.
16 T. G. Leong, C. L. Randall, B. R. Benson, A. M. Zarafshar and D. H. Gracias, *Lab Chip*, 2008, **8**, 1621.
17 J. El-Ali, P. K. Sorger and K. F. Jensen, *Nature*, 2006, **442**, 403.